www.ijecs.in
International Journal Of Engineering And Computer Science
Volume 14 Issue 07 July 2025, Page No. 27531-27546
ISSN: 2319-7242 DOI: 10.18535/ijecs/v14i07.5190

Frequency Reconfigurable Fractal Microstrip Filtering Antenna for Cognitive Radio Applications

G. Mohan[1], M. Pranay Kumar[1], K. P. Vinay[2], Ramesh Boddu[*2]

Department of ECE, Chaitanya Deemed to be University, Warangal, Telangana, India[1]
Department of ECE, Raghu Engineering College, Visakhapatnam, A.P, India[2]

Abstract
Tunable microstrip filtering antennas can be used to modify the operating frequency, polarization, or radiation pattern in real time. These antennas provide a number of advantages, such as more flexibility and adaptability and decreased dimensions, weight, and power consumption. The main aim of the current work is to design a tunable microstrip filtering antenna for cognitive radio applications. Prior to tune the frequency of the proposed design the operating bandwidth is enhanced by implementing the Snow-flake Koch fractal optimization of 3rd iteration along with the defected ground structure. To achieve the frequency tunable characteristics a stepped impedance resonator (SIR) filter is integrated with the feed line. The order of the SIR filter is responsible for frequency tunability. At each stage the simulated designs are fabricated and measured using VNA and anechoic chamber. The peak gain achieved is 3.2dBi whereas the minimum gain achieved is 1.7dBi. The co-polarization values are 25dB is stronger than cross-polarization values. There is a good concurrence is observed between the simulated and measured results in terms of 10dB Return Loss, VSWR, Gain, Directivity and Far Filed radiation patterns. The proposed design is well suited for cognitive radio applications as it is operating at 1.97GHz, 3.97GHz and 5.87 GHz frequencies respectively.

Keywords: Microstrip antenna, Defected Ground Structure, fractal design, filtering antenna, SIR filter

1.Introduction

The Cognitive Radio system, which monitors the spectrum and redistribute services to unoccupied frequency channels, has gained attention for its potential to improve the efficiency of the spectrum. Wireless communication is in high demand today, and antennas play a crucial role in it. An antenna works as a transducer, converting electromagnetic (EM) waves into signals and vice versa [1]. The microstrip antenna is well suited to integrate with the VLSI circuit boards due to its low profile, less cost and planar structure. An antenna with a specific frequency and radiation pattern is typically suited for only one application. Therefore, devices needing multiple radio applications often require multiple antennas. Using more antennas requires more space, increases the chance of interference between them, raises installation costs, and complicates device design. Therefore, it is needed to design an antenna with wide operating bandwidth [2]. Over the past two centuries, there has been a significant amount of advancement and research towards increasing the bandwidth and merging many antennas into a single device. To achieve the broad bandwidth many techniques have been implemented in the literature like using proximity coupling feed [3], implementation of parasitic patch [4], modifying the shape of the patch [5], and using array structures [6-9] which inherently increases the design complexity, size enlargement and fabrication losses.

One of the promising technique is fractal patterns that are integrated in microstrip patch antennas to considerably reduce antenna size, enhance the bandwidth, and increase electromagnetic radiations throughout the whole surface volume. These fractal structures are often inspired by natural codes that repeat themselves at different sizes. The fractal structures utilizes the Iterated Function System (IFS), it is a

traditional fractal generation approach that creates self-similar structures with certain vertices. Many fractal geometries are mentioned in the literature like Sierpinski carpet and gasket [10-14], Minkowski gasket fractal [15-19], Hilbert's Fractal [20-23], Peano's Fractal [24-26], Crinkle Shaped fractal [27-28], Koch fractal [29-31]. The above mentioned fractal geometries are the deterministic fractals, which can be used to create a scaled-down design with a recursive algorithm. But, the above mentioned fractal shapes reduces the patch size by 18%, 32%, 15%, 42%, 30% and 47% for Sierpinski carpet, Sierpinski gasket, Minkowski curve, Hilbert's Fractal, Peano's Fractal, Crinkle Shaped fractal geometries respectively. The modified Koch Snowflake fractal structure is chosen, because it specifically reduces the patch size by 56% by forming inside a triangle since the supplemental triangles formed in the subsequent iterations will fall within the same bigger triangle. But, such broadband antennas seriously causes the lot of interference to the nearby systems.

Since, scientists are now interested in tunable antennas to support various wireless services, meet emerging needs, and adapt to dynamic environments without creating interference to the nearby systems. In order to provide several functions, tunable antennas have various customizable primary features, such as operating frequency, the bandwidth, radiation pattern, polarization, and so on. These tunable antennas uses Radio-Frequency (RF) switches, mechanical actuators and active components like PIN diodes [32-34], RF-MEMS [35-38] and varactor diodes [39] into the design to achieve frequency tunability. Due to the involvement of the active and passive components in the antenna designs will be capable of supporting many wireless applications like Bluetooth, UMTS, Wi-MAX and Wi-Fi etc. simultaneously without causing the interference to the nearby systems [40-42]. But, these RF switches, actuators, PIN diodes and varactor are integrated with the radiating element which increases the fabrication losses, connection losses and unnecessary metallization leads to fringing effects [43]. However, due to the involvement of these active elements increases the overall cost and extra circuitry increases the size of the antenna [44]. In recent years, several tunable microstrip BPFs have been introduced to design a compact, efficient, and reconfigurable planar filters with a wide tuning. These are very useful since they may be printed directly on the dielectric substrate materials. There is no need of designing the microstrip antenna and filter separately rather, the filter is joined directly to the patch resulting in more compact structures and improving the entire performance of the RF and MW systems [45]. To achieve the tunable characteristics, compactness, without increasing the fabrication losses the 3rd order SIR filter is designed and integrated with the radiating element.

In this article, a frequency tunable microstrip filtering antenna is proposed for cognitive radio applications and is structured in following way: The design and implementation is presented in section 2. The section two having 3 subsections which is implemented in 3 steps. In step-1, the design of microstrip antenna is presented, fractal optimization is implemented in Step-2 and the implementation of tunable filtering antenna is presented in Step-3. The results of each design is also explained in section-3. Finally section 4 concludes prime investigations and future of the work.

2. Design and Implementation

The proposed tunable filtering antenna design is presented in 3 steps. In the first step the design a basic microstrip patch antenna with defected ground structure is presented. To increase the operating bandwidth and to reduce the unnecessary metallization in the radiation patch the radiation element is implemented with modified Snowflake-Koch fractal optimization and is presented in the second step. Further, to achieve the frequency tunability the proposed design is integrated with Stepped Impedance Resonator (SIR) filter and is presented in the third step.

2.1Step-1: Design of Basic Antenna

In step-1, the proposed microstrip antenna is designed using low cost FR4 substrate with ε_r of 4.4 with tanδ is 0.002 having the overall size of $32\times 45 \times 1.6mm^3$. The simple square shaped patch and microstrip line feed is used due to their simple structures. Initially, the substrate is backed with complete ground plane. Later, the ground plane is implemented with Defected Ground Structure (DGS) and its length is optimized to achieve the better operating bandwidth.

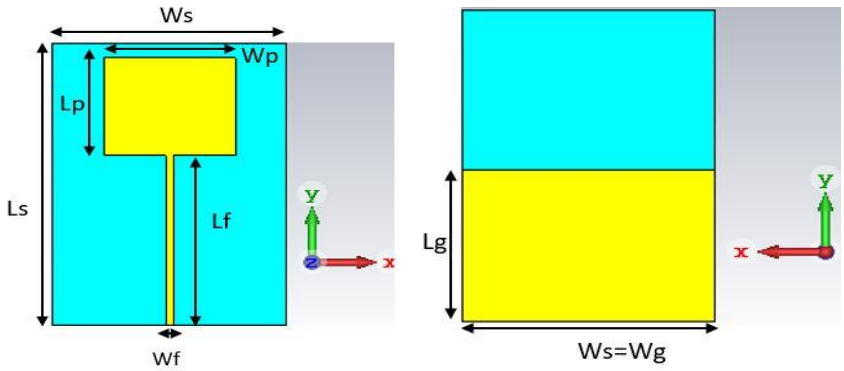

(a) Simulated view of basic microstrip antenna design

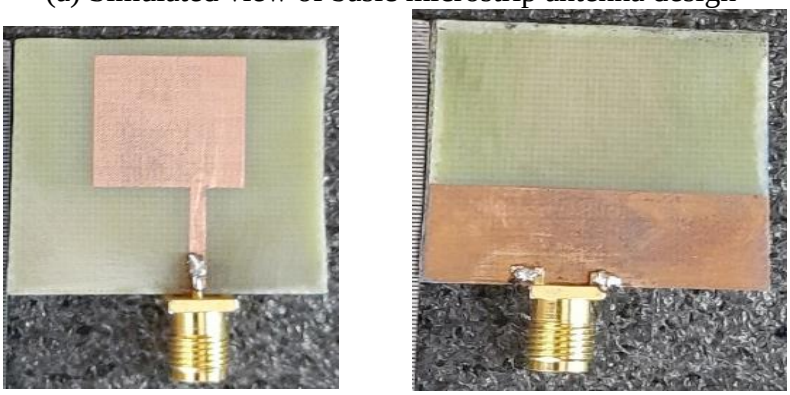

(b) Fabricated view of basic microstrip antenna design

Fig. 1 Simulated & Fabricated designs of the basic microstrip antenna

The proposed design is implemented using 3D electromagnetic simulation tool CST microwave studio. The proposed design is fabricated and tested using Vector Network Analyser (VNA) and Anechoic chamber. The simulated and fabricated designs are indicated in Fig. 1. Fig. 1(a) depicts the simulated top and bottom views of the proposed basic antenna and Fig. 1(b) shows the top and rear views of the fabricated basic microstrip antenna. The optimized dimensions of the proposed basic microstrip antenna is tabulated in Table 1. The length of the defected ground structure is optimized for better operating characteristics.

Table 1 Dimensions of the proposed basic microstrip antenna

S. No	Parameter	Value (mm)
1	Ws	32
2	Ls	45
3	Lf	27
4	Wf	1
5	Lp	15.6
6	Wp	18
7	Wg	32
8	Lg	22

2.2 Step-2: Design of Fractal Antenna

In the design step-2, the basic square shaped patch antenna is implemented with modified Snowflake-Koch fractal structure. The modified Snowflake-Koch fractal can be constructed using the following mathematical equations. The equilateral triangle with each side length is (L) and considered it as 0^{th} iteration. For 1^{st} iteration, divide each side into 3 equal parts (L/3). Replace the middle segment with two segments of lengths L/3, forming an equilateral triangle and follow the same procedure for remaining two sides of the n triangle. Repeat the same procedure for further iterations.

Let $V_0(X) = X$ (0^{th} iteration) (1)

$V_1(X) = (1/3)\ X + (1/3)$ (1^{st} iteration) (2)

$$V_2(X) = (1/9)\ X + (2/9) + (1/9)\ X\ (2^{nd}\ \text{iteration}) \quad (3)$$

…..

$$V_n(X) = (1/3)^n\ X + \ldots\ (n^{th}\ \text{iteration}) \quad (4)$$

By the use of above equations the basic shaped patch is optimized using fractal optimization up to 3 iterations. The fractal shape is initially started with square shape, then its shape is modified to triangular in 1st iteration. The simulated fractal microstrip antenna with Snowflake-Koch fractal optimization is shown in Fig. 2.

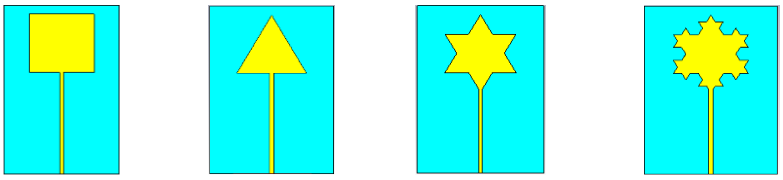

0th iteration 1st iteration 2nd iteration 3rd iteration

Fig. 2 Simulated view of fractal microstrip antenna up to 3 iterations

For every iteration the size of the radiating element is reduced by 1/3rd value of the original dimension. Here, the modified Snow-flake fractal optimization technique is implemented. In this optimization technique the initial shape should be triangular shape to optimize 1/3rd value in each iteration. But in the proposed design the shaped of the patch is square, therefore a novel technique is implemented by modifying the optimization value for the first iteration and it is mentioned as modified snowflake fractal optimization technique. To test concurrence the final i.e. 3rd iterated fractal structure is fabricated and measured. The simulated and measured designs of the fractal microstrip antenna for 3rd iteration is shown in Fig. 3 and the measurement setup with vector network analyser is shown in Fig. 4.

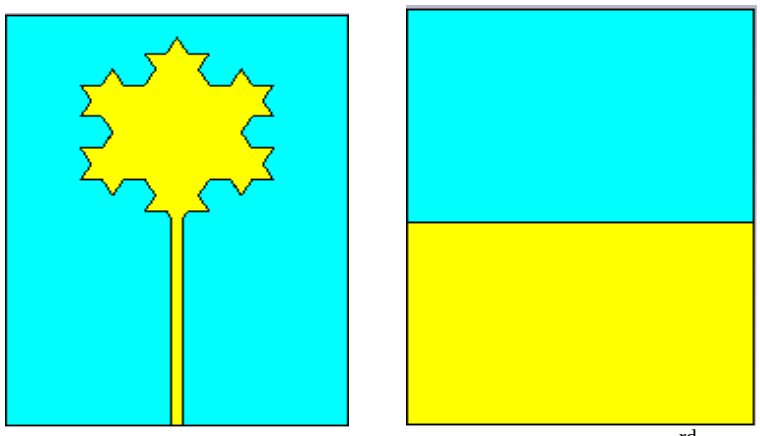

(a) Simualted design of fractal microstrip antenna after 3rd iteration

(b) Fabricated design of fractal microstrip antenna after 3rd iteration

Fig. 3 The simualted & fabricated designs of the proposed fractal microstrip antenna

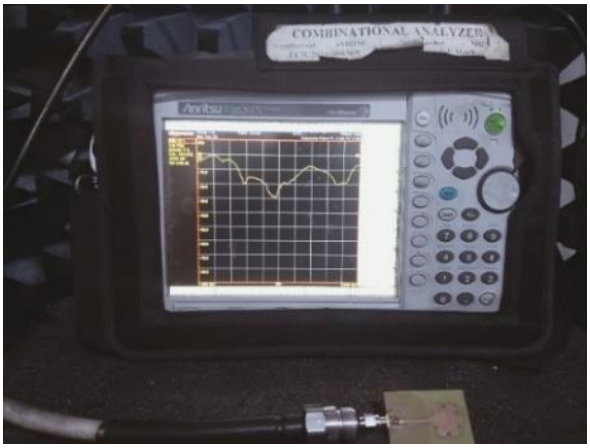

Fig. 4 Measurement setup with VNA

2.3 Step-3: Design of Filtering Antenna

Now a days, the microstrip antennas with tunable frequency characteristics is extremely required. In the wide operating band if antenna can be tuned in terms of frequency then it is very much flexible to alter the operating frequency. Due to this interference caused by nearby systems is reduced without of changing the physical design. To achieve the tunable characteristics the proposed fractal patch is integrated with SIR filter. The SIR filter can be considered as two transmission lines of different lengths and characteristic impedance as shown in Fig. 5. Its design transmission line can be controlled by the alternating segments of high and low characteristics impedance lines. The condition of resonance for SIR filter is given by

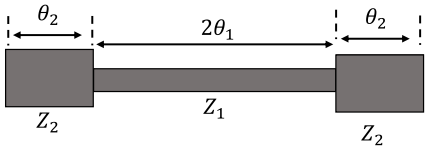

Fig. 5 SIR filter with different impedance values

$$G = \frac{\tan\theta_1 * (\tan\theta_T - \tan\theta_1)}{1 + \tan\theta_T \tan\theta_1} \quad \ldots\ldots (5)$$

$$\theta_1 = \beta_1 l_1 \quad \ldots\ldots\ldots\ldots\ldots\ldots (6)$$

$$\theta_T = \theta_1 + \theta_2 \quad \ldots\ldots\ldots\ldots\ldots (7)$$

$$\theta_2 = \theta_1 = \tan^{-1}\left(\frac{2\sqrt{G}}{1-G}\right) \quad \ldots\ldots\ldots (8)$$

By the use of above equations the location and length of the arms of the filter is calculated and integrated with microstrip line feed. To select the operating frequency from the broad band the order of the SIR filer is increased. To select single frequency first order SIR filter is integrated. To select dual and triple bands the order is increased to 2nd and 3rd orders. The simulated design of tunable microstrip filtering antenna with SIR filter is shown in Fig. 6. Fig. 6 (a) shows the microstrip filtering antenna with 1st order SIR filter and Fig. 6 (b) & (c) shows the 2nd & 3rd order microstrip filtering antenna designs.

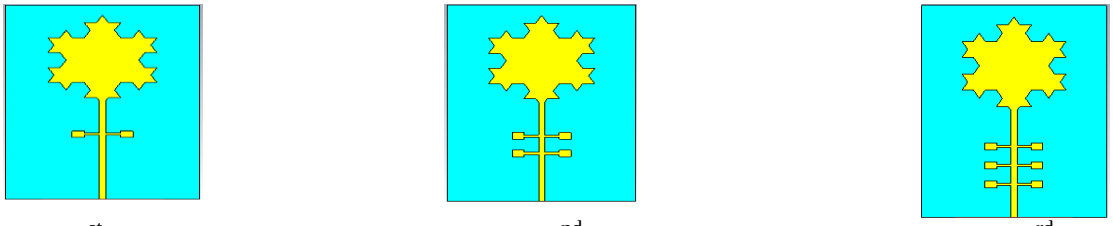

(a) 1st order (b) 2nd order (c) 3rd order

Fig. 6 Top view of the simulated microstrip filtering antenna with SIR filter

The 3rd order microstrip filtering antenna with SIR filter is fabricated and the simulated and fabricated designs are depicted in Fig. 7.

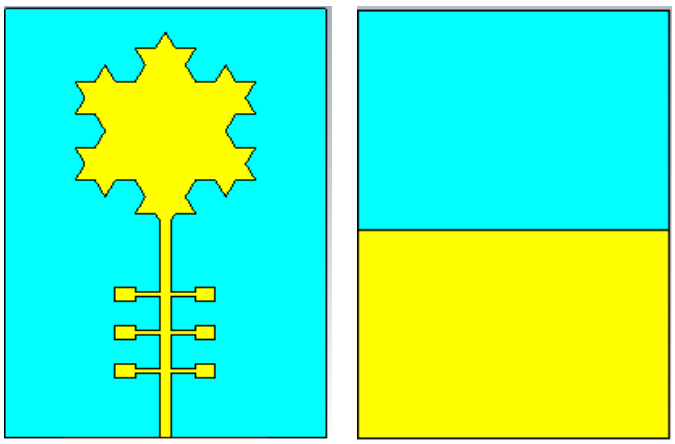

(a) Simulated design

b) Fabricated design

Fig. 7 Simulated & fabricated microstrip filtering antenna

3. Results & Discussion:

The simulated and measured S_{11} plot of the basic microstrip antenna is depicted in Fig. 8. The measured return loss is very close to the simulated value. The operating frequency of the basic microstrip antenna is from 2.3GHz to 4GHz with minimum S_{11} of -20.38dB at 3GHz.

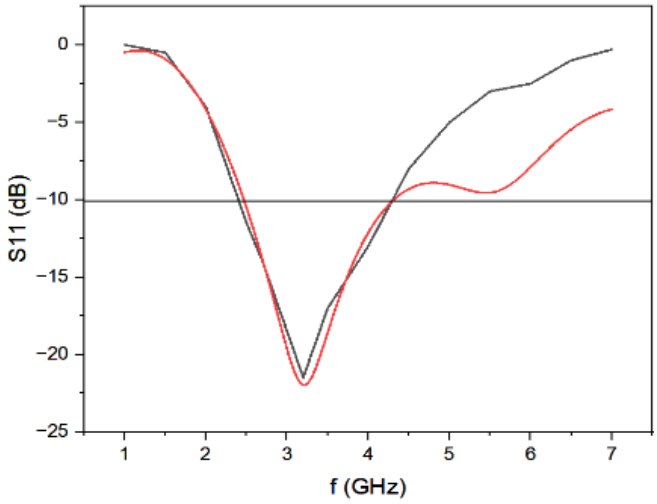

Fig. 8 S_{11} plot of the basic microstrip antenna

The comparison of simulated and measured gain plot of the proposed basic microstrip antenna is depicted in Fig. 9. The peak gain achieved is 1.7dB at centre frequency of 3GHz. There is very good agreement is observed between the simulated and measured gain values.

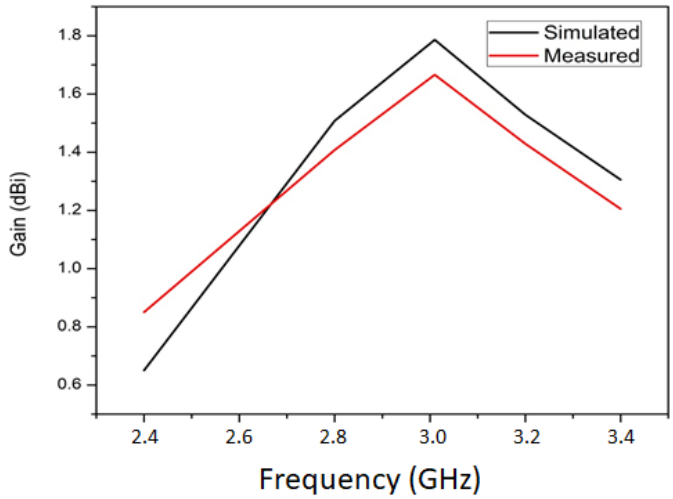

Fig. 9 Simulated & Measured gain plot of the basic microstrip antenna

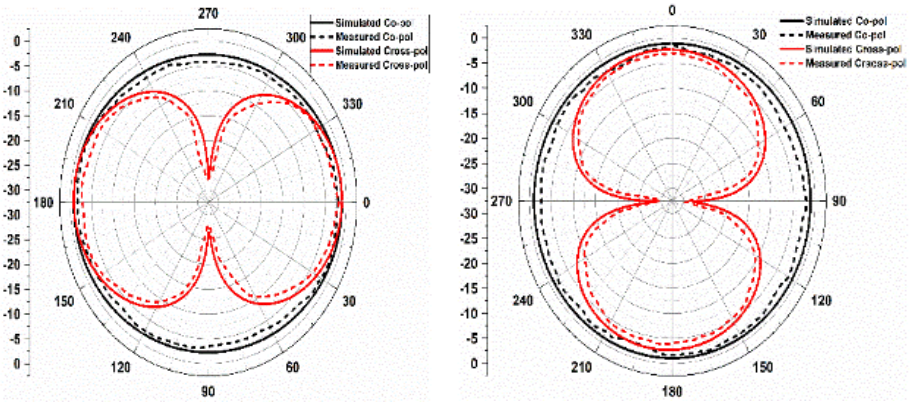

(a) E-Plane (b) H-Plane

Fig. 10 Simulated and measured Radiation patterns of basic microstrip Antenna

Fig. 10 shows the simulated and measured radiation patterns at 3GHz for basic microstrip antenna. The measured results well agree with the simulated results. From the measured and simulated radiation patterns it is clearly observed that the co-polarization is 20dB stronger than the cross-polarization values.

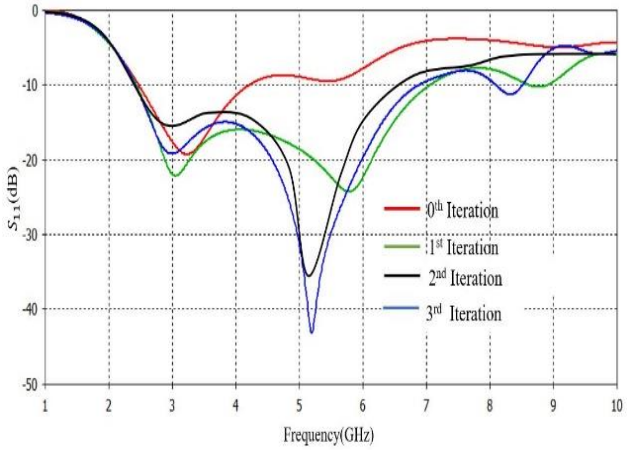

Fig. 11 S_{11} plot of the fractal microstrip antenna for 4 iterations

To increase the operating bandwidth of the basic design the modified snow-flake fractal optimization is applied on the radiating patch up to 3 iterations. The S_{11} plot of the fractal microstrip antenna for each iteration starting from 0^{th} to 3^{rd} order is shown in Fig. 11. From the plot it is clearly observed that the operating bandwidth is increasing with the increasing with number of iterations. The wideband is achieved for 3^{rd} iteration which was indicated in blue colour in the Fig. 11. For the 0^{th} & 1^{st} iterations the operating frequency is almost same i.e., 2.3GHz-4GHz with the bandwidth of 1.69GHz. Whereas, for the 2^{nd} & 3^{rd} iterations the bandwidth achieved is 4.458GHz with operating frquency varying from 2.42GHz-7GHz. But, in the 3^{rd} iteration the minimum S_{11} = -43.16dB is achieved at 5.1GHz frequency. The iteration value is increased further which leads to fabrication losses.

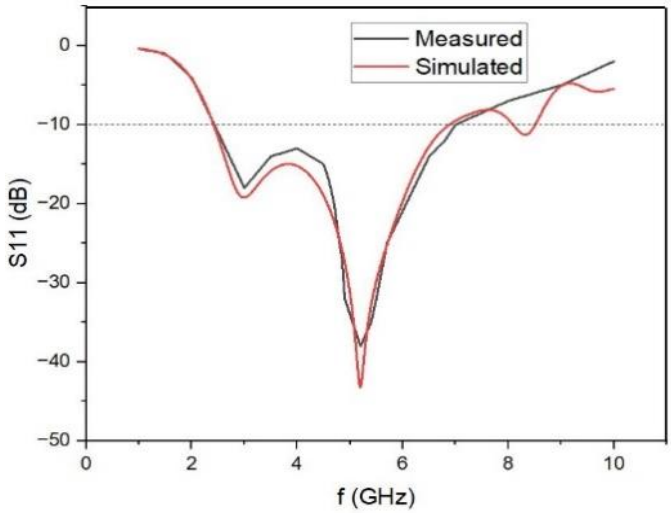

Fig. 12 The comparision of S_{11} plot of the simulated and fabricated fractal antenna

The S_{11} plot of the simulated and measured fractal microstrip antenna is shown in Fig. 12. The measured result is almost coincides with the simulated result. The operating frequency of the 3^{rd} order fractal microstrip antenna attained is 2.43GHz-7GHz with the bandwidth of 4.4GHz. The measured values are well agreeing with the simulated values.

The simulated and measured VSWR plot of the proposed fractal microstrip antenna is shown in Fig. 13. From the VSWR plot it is observed that both simulated and measured values are well below 2 for the entire operating band i.e, from 2.4GHz-7GHz.

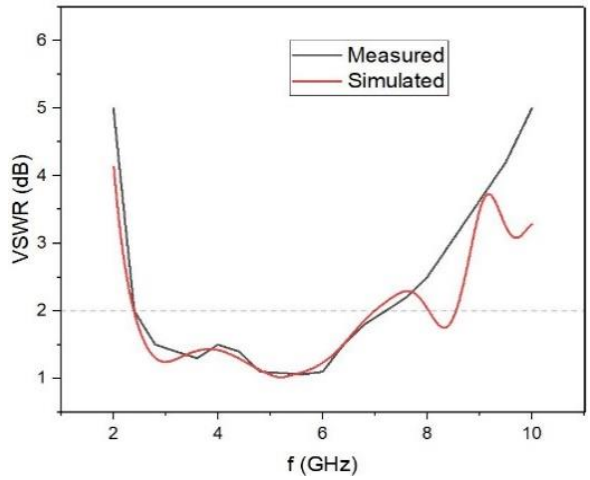

Fig. 13 Simulated and measured VSWR plot of the fractal microstrip antenna

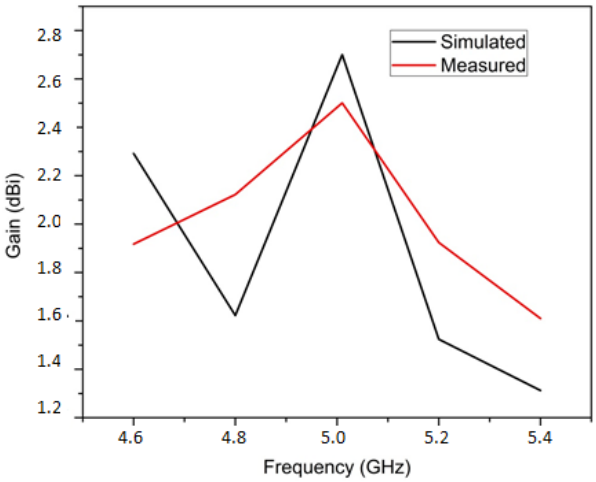

Fig. 14 simulated and measured gain plot of the fractal microstrip antenna

The simulated and measured gain plot of the fractal microstrip antenna is shown in Fig. 14. The measured gain is close to the simulated gain. The peak simulated gain of the fractal antenna is 2.71 dB at 5.1 GHz whereas the measured gain is 2.53dB at the same frequency. It is clear that both the simulated and experimental antennas provide a wider bandwidth and show that they are in reasonable agreement with each other.

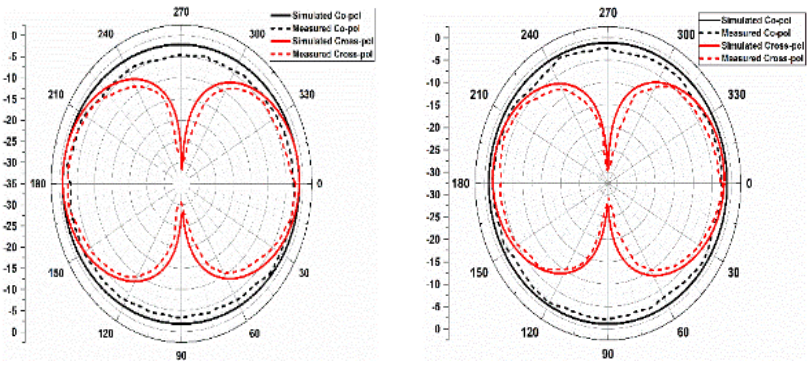

(a) E-Plane (b) H-Plane

Fig. 15 Simulated & Measured radiation patterns of the two principle planes

Fig. 15 shows the simulated and measured radiation patterns at 5.1GHz of the fractal microstrip antenna. It is observed that the measured results agrees well with the simulated results.

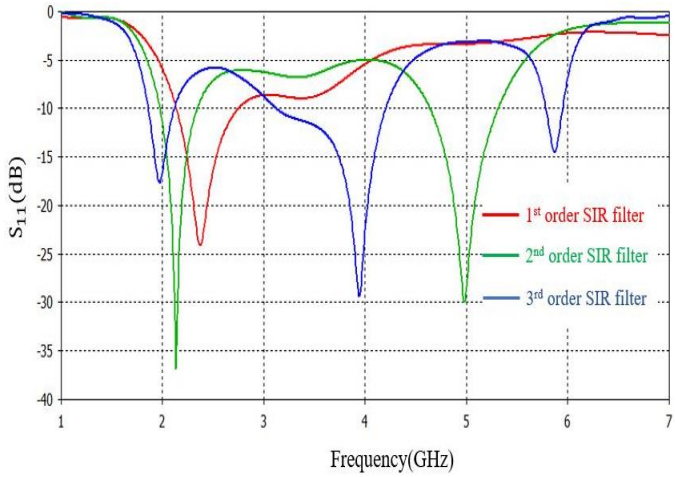

Fig. 16 comparison of S_{11} plots of the microstrip filtering antenna

To tune the operating frequency from the broadband the SIR filter is attached with the feed line. The simulated S_{11} plot of the microstrip filtering antenna for all 3 orders is shown in Fig. 16. From the figure it is clearly observed that the single band is selected if 1st order SIR filter is attached with feed line. The operating frequency of filtering antenna with 1st order SIR filter is 2.2GHz-2.8GHz which is useful to utilize the antenna for Bluetooth applications. The dual band of operation is achieved if another SIR filter is integrated with feed line of fractal microstrip antenna. The operating frequencies of the filtering microstrip antenna with 2nd order SIR filter is given by 2GHz-2.43GHz and 4.8GHz-5.2GHz. This design can used for Bluetooth applications as well as WLAN applications. The triple band of operation is achieved by integrating third SIR filter with the feed line. The operating frequencies are given by (1.8-2.12) GHz, (3.1-4.2) GHz & (5.78- 5.95) GHz respectively. This design is well suitable for cognitive radio applications.

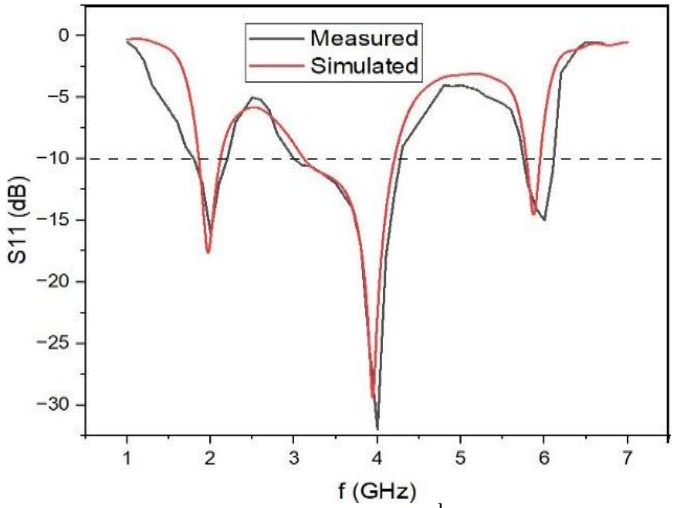

Fig. 17 Simulated and measured S_{11} plot of the 3rd order microstrip filtering antenna

The simulated and measured S_{11} plot of 3rd order of microstrip filtering antenna is shown in Fig. 17. There is a very good agreement is observed between the simulated and measured values. Therefore, by increasing the number of the SIR filter the tuning of operating frequency is increased from single band of operation to triple band of operation. As it is getting band notch characteristics the interference caused by nearby systems can be reduced to extreme possible level. Therefore the proposed tunable microstrip filtering antenna is very much suitable to use for the cognitive radio applications.

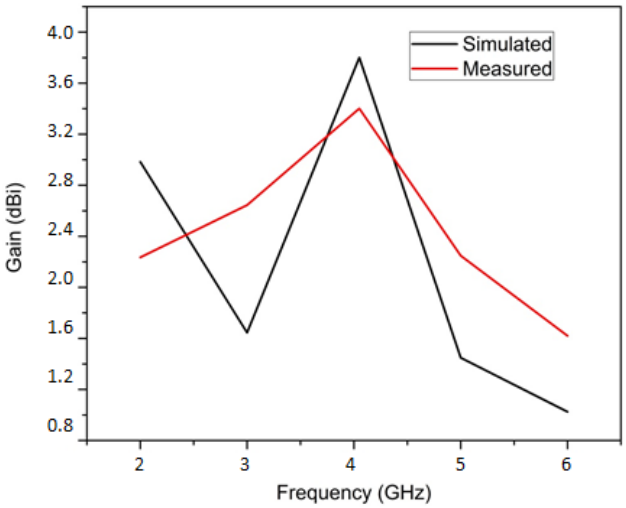

Fig. 18 Simulated & Measured gain plot of 3rd order microstrip filtering antenna

The simulated & measured gain plot of the 3rd order filtering antenna is shown in Fig. 18. The peak gain values of the proposed filtering antenna is 2.3dBi, 3.2dBi and 1.83dBi at 1.97GHz, 3.97GHz and 5.87GHz respectively. The peak gain is observed is 2.92dBi at 3.97GHz. Here, in this case also the measured values are well agreeing with the simulated values.

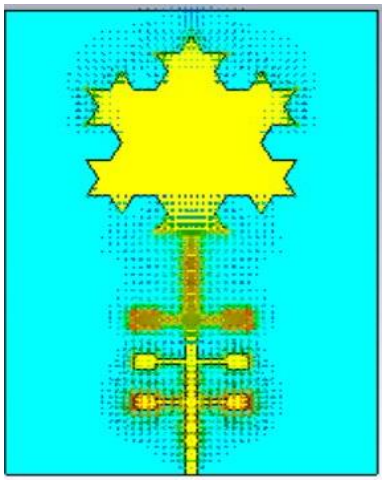

Fig. 19 Surface current distribution of the filtering antenna

The surface current distribution of the tunable filtering antenna with 3rd order SIR filter is shown in Fig. 19. The effect of the filter on the current distribution is clearly observed. The maximum current is concentrated at the edges of the patch.

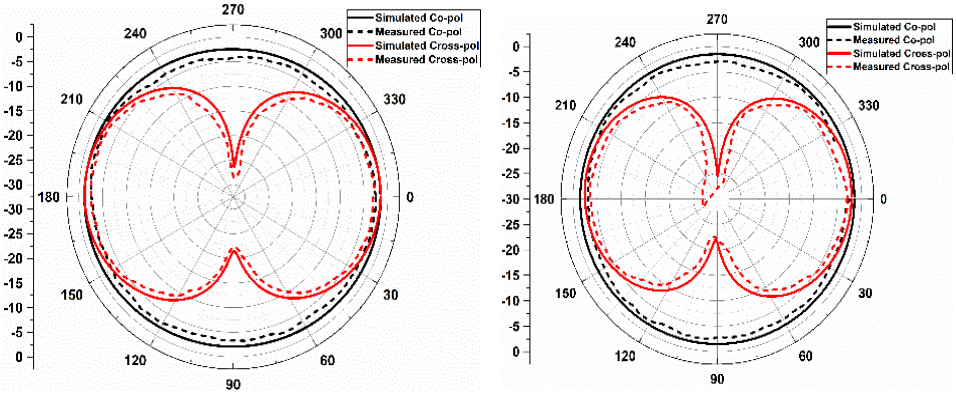

(a) E-Plane (b) H-Plane

Fig. 20 Simulated & Measured E & H-Plane Radiation patterns of the filtering antenna

The Simulated and measured E & H-Plane radiation patterns of the 3rd order microstrip filtering antenna is shown in Fig. 20. It is observed that co-polarization values are at least 25dB stronger than the cross polarization values. There is very good agreement is observed between the simulated and measured results.

Table 2 comparison of proposed work with some recent works

S. No	Reference	Overall Size (mm^3)	UWB coverage (GHz)	Narrow band coverage (GHz)
[40]	(I. Ahmad et al., 2021)	27 × 30 × 1.6	2 to 7.65	2.6; 3.5; 4.2; 4.5; 5; 5.5
[41]	(A. A. Palsokar et al., 2020)	58 × 66 × 1.6	2.1 to 10.6	2.47; 3.8; 5.36
[42]	(G. Singh et al., 2020)	29 × 34 × 1.5	1.2 to 8	1.8; 2.1; 2.2; 2.4; 2.6; 3.5; 4;5
[43]	(A. Ghaffar et al., 2021)	40 × 50 × 1.6	1.1 to 5.7	1.8; 2.1; 2.4
[44]	(Madhav, B. T. P et al., 2018)	58×48×1.6	2 to 6	2.3, 2.4, 2.5
[45]	(Iqbal, A., S et al., 2018)	39 × 37 ×1.6	2 to7	2.45, 3, 5.2
- -	Proposed work	32 × 45 × 1.6	1.8-7.0	1.8 to 2.12, 3.1 to 4.2, 5.78 to 5.95

4. Conclusion and future work

This article presents the tunable microstrip filtering antenna for cognitive radio applications. The tunability is achieved by increasing the order of the SIR filter. For 1st order the proposed design is tuned to single frequency centred at 1.97GHz. Adding another SIR filter the proposed antenna is configured to dual frequencies i.e., at 1.97GHz and 3.97GHz. Triple band of operation is achieved with 3rd order filter. All the final designs in each type is fabricated and tested. For the all designs the simulated results are well agreeing with measured results. The proposed design is operating at 3 different frequency bands the proposed antenna is very much suitable cognitive radio applications. In future, this work may be extended for quad band of operations or for multi band of operation.

Conflicts of interest

The authors have no conflicts of interest to declare.

References

1. Kin-Ln Wong. Compact and Broadband Microstrip Antennas. John Wily & Sons by; 2002.
2. Girish Kumar. Broadband Microstrip Antennas. Artech House, INC; 2003.
3. Pozar. D.M and Kaufman. B. Increasing the bandwidth of a microstrip antenna by proximity coupling. Electronic Letters. 23(2); 1987:368-369.
4. Tseng. C.F, Huang. C. L, Hsu. H.C. Microstrip Fed Monopole Antenna with a Shorted Parasitic Element for Wideband Application. Progress in Electromagnetics Research Letters. 7; (2009):115-125.
5. Islam. M.T. Broadband E-H Shaped Microstrip Patch Antenna for Wireless Systems. Progress in Electromagnetics Research, PIER. 98, (2009):163–173.

6. Li, H, Wang. B. H, and Shao. W. Novel broadband reflector array antenna with compound-cross-loop elements for millimetre wave application. Journal of Electromagnetic Waves and Applications. 21(10), (2007):1333–1340.
7. Ershadi. S, Keshtkar. Abdelrahman. A. H, and Xin. H. Wideband High Gain Antenna Subarray for 5G Applications. Progress in Electromagnetics Research C. 78; (2017):33-46.
8. Jeyakumar. P. Design and Simulation of Directive High Gain Microstrip Array Antenna for 5G Cellular Communication. Asian Journal of Applied Science and Technology. 2(2), (2018):301-313.
9. Kavitha. M. 28 GHz Printed Antenna for 5G Communication with Improved Gain Using Array. International Journal of Scientific & Technology Research. 9(3); (2020):5127-5133.
10. Oraizi. H and Hedayati. S. Miniaturized UWB monopole microstrip antenna design by the combination of Giusepe Peano and Sierpinski carpet fractals. IEEE Antennas Wireless Propagation Letters. 10; (2011):67–70.
11. Shrestha. S, Park J.J, Noh S.K and Choi D.Y. Design of 2.45 GHz Sierpinski fractal based miniaturized microstrip patch antenna. In Proceedings of the 2012 18th Asia —Pacific Conference on Communications.2012 (pp. 36–41).
12. Herbko. M and Lopato.P. Microstrip patch strain sensor miniaturization using Sierpinski curve fractal geometry. Sensors. 19;(2019):3989.
13. Reha A, El Amri. A and Bouchouirbat. M. The behavior of CPW-fed Sierpinski curve fractal antenna. Journal Microwave Optoelectronics Electromagnetics Applications. 17; (2018):366–372.
14. Tiwari. D, Ansari. A. J, Saroj. K.A and Kumar M. Analysis of a miniaturized hexagonal Sierpinski gasket fractal microstrip antenna for modern wireless communications. AEU–International Journal of Electronics Communication. 123; (2020):153288.
15. Liu. J.C, Liu. H.H, Yeh.K.D, Liu. C.Y, Zeng. B. H and Chen. C.C. Miniaturized dual-mode resonators with Minkowski-island-based fractal patch for WLAN dual-band systems. Propagation Electromagnetic Research. 26; (2012):229–243.
16. Nugraha. D.E.P.I, Surjati. I and Alam. S. Miniaturized Minkowski-island fractal microstrip antenna fed by proximity coupling for wireless fidelity application. Telecommunications Computer Electronic Control. 15, (2017):1119–1125.
17. Ali. K. J and Ali. J. A. S. A miniaturized multiband Minkowski-like pre-fractal patch antenna for GPS and 3G IMT-2000 handsets. Asian journal of Information Technology. 6,(2007):584–588.
18. Costanzo. S and Qureshi. A. M. Miniaturized planar inverted-F antenna using Minkowski pre-fractal structure. In Proceedings of the 2010 14th European Conference on Antennas and Propagation. 2020 (pp.199-204).
19. Oliveira. E. E. C., Silva. P. H. D. F, Campos. A. L. P. S. Small-size quasi-fractal patch antenna using the Minkowski curve. Microwave Optical Technology Letters. 52, (2010):805–809.
20. Tarbouch. M, Amri. A. El, Terchoune. H and Barro. O. Compact CPW-fed microstrip octagonal patch antenna with Hilbert fractal slots for WLAN and WIMAX applications. Innovations in Smart Cities and Applications, Lecture Notes in Networks and Applications.2018 (pp. 432–444).
21. Kumar. A and Pharwaha. A. P. S. Development of a modified Hilbert curve fractal antenna for multiband applications. IETE journal of Research.2020.
22. Samson Daniel. R. Asymmetric coplanar strip fed with Hilbert curve fractal antenna for multiband operations. Wireless Personal Communications. 116, (2021)791– 803.
23. Huang. J. T, Shiao. J. H, and Wu. J. M. A miniaturized Hilbert inverted-F antenna for wireless sensor network applications. IEEE Transactions Antennas Propagation. 58, (2010):3100–3103.
24. McVay. J and Hoorfar. A. Miniaturization of top loaded monopole antennas using Peano-curves. In Proceedings of the 2007 IEEE Radio and Wireless Symposium.2007 (pp. 253–256).
25. Oraizi. H, Bahramgiri. M and Hedayati. S. A novel miniaturized multilayer E-shaped patch antenna using Giuseppe Peano fractal geometry on its edges for WLAN dual band applications. In Proceedings of the 2013 21st Iranian Conference on Electrical Engineering. 2013.

26. Sharma. N, Pal Singh. G and Sharma. V. Miniaturization of fractal antenna using novel Giuseppe Peano geometry for wireless applications. In Proceedings of the 1st IEEE International Conference on Power Electronics, Intelligent Control and Energy Systems. 2016 (pp. 1–4).
27. Beigi. P and Mohammadi. P. A novel small triple-band monopole antenna with crinkle fractal structure. AEU – International Journal of Electronics Communication. 70, (2016):1382–1387.
28. Beigi. P, Zehforoosh. Y, Rezvani. M and Nourinia. J. Evaluation of a compact triangular crinkle-shaped multiband antenna with circular polarized for ITU band based on MADM method. Circuit World. 45, (2019):292–299.
29. Campos. A. L. P. S, de Oliveira E. E. C and Silva P. H. F. Miniaturization of frequency selective surfaces using fractal Koch curves. Microwave Optical Technology Letters. 51, (2009):1983–1986.
30. Manohar. M. Miniaturised low-profile super wideband Koch snowflake fractal monopole slot antenna with improved BW and stabilised radiation pattern. IET Microwave Antennas Propagation. 13, (2019):1948–1954.
31. Khan. O. M, Islam Z. U, Rashid. I, Bhatti F. A, and Islam. Q. U. Novel miniaturized Koch pentagonal fractal antenna for multiband wireless applications. Progress in Electromagnetic Research. 141, (2013):693–710.
32. El-Tanami. M. A. and Rebeize. G. M. Corrugated microstrip coupled lines for constant absolute bandwidth tunable filters. IEEE Transaction on Microwave Theory Techniques. 56 (5), (2008):1137–1148.
33. Zhang. X. Y, Xue. Q, Chan. C. H, and Hu. J. B. Low-loss frequency-agile bandpass filters with controllable bandwidth and suppressed second harmonic. IEEE Transactions on Microwave Theory Techniques. 58 (6), (2010):1557–1564.
34. Peng. W. W and I. C. Hunter .I.C. A new class of low-loss high-linearity electronically reconfigurable microwave filter. IEEE Transactions on Microwave Theory Techniques. 56 (8), (2008):1945–1953.
35. Blondy. P, C. Palego. C, Houssini. M, Pothier. A, and Crunteanu. A. RF-MEMS reconfigurable filters on low loss substrates for flexible front ends. Proceeding Asia-Pacific Microwave Conference (APMC).2007. (pp.1–3), Bangkok.
36. Reines, I. C, Goldsmith C. L, Nordquist. C. D, Dyck C. W, G. Kraus. M, Plut. T. A, Finnegan. P. S, Austin. F, and Sullivan. C. T. A low loss RF MEMS Ku-band integrated switched filter bank. IEEE Microwave Wireless Components Letters. 15 (2), (2005):74–76.
37. Zhang, N., Deng. Z. L, and Sen. F. CPW tunable band-stop filter using hybrid resonator and employing RF MEMS capacitors. IEEE Transactions on Electron Devices; 60 (8), (2013):2648–2655.
38. Safari. M, Shafai.C and Shafai. L. X-band tunable frequency selective surface using MEMS capacitive loads. IEEE Transactions on Antenna and Propagation. 15(4); (2014):1–9.
39. Chun. Y. H, Hong. J. S, Peng. B, Jackson. T. J, and Lancaster. J.M. BST varactor tunable dual-mode filter using variable Zc transmission line. IEEE Microwave and Wireless Components Letters. 2008; 18(1):167–169.
40. Ahmad. I, Haris. D, Wasi Khan and Syed Amir. A. S. Design and experimental analysis of multiband compound reconfigurable 5G antenna for sub-6 GHz wireless applications. Wireless Communications and Mobile Computing. 2021(pp.1–14).
41. Palsokar. A. A and Lahudkar. S. L. Frequency and pattern reconfigurable rectangular patch antenna using single PIN diode. AEU - International Journal of Electronics and Communications. 2020; 125:153-157.
42. Singh. G, Kanaujia. K. B, Pandey. V. K, Gangwar. D, and Kumar. S. Pattern and frequency reconfigurable antenna with diode loaded ELC resonator. International Journal of Microwave and Wireless Technologies. 2020; 12(2):163–175.
43. Ghaffar. A, Li. J. X, Awan. A. W, Hussain. A. A flexible and pattern reconfigurable antenna with small dimensions and simple layout for wireless communication systems operating over 1.65–2.51 GHz. Electronics.2021; 10(5):601-606.

44. Madhav, B. T. P., Rajiya. S, Nadh. B.P, and Kumar. S. M. Frequency reconfigurable monopole antenna with DGS for ISM band applications. Journal of Electrical Engineering. 2018; 69(4):293–299.
45. Iqbal, A., S. Ullah, U. Naeem, A. Basir, and U. Ali, Design, fabrication, and measurement of a compact frequency reconfigurable modified T-shape planar antenna for portable applications, Journal of Electrical Engineering and Technology, 2017;12(4):1611–1618.

G. Mohan is a Research Scholar in the Department of Electronics & Communication Engineering at Chaitanya Deemed to be University, Hyderabad, India. He received his M.Tech in Electronics & Communication Engineering (VLSI) from JNTU University, Hyderabad, and his Bachelor's degree in Electronics & Communication Engineering from the JNTU of Hyderabad India.

M. Prany Kumar is Ph.D. in Electronics & Communication Engineering at from University of Allahabad India.. He is currently working as Associate Professor in the department of ECE, Chaitanya Deemed to be university warangal. He is professional membe. He receieved his M. Tech in Electronics & Communication Engineering (Embedded Systems) from JNTUH, and his Bachlor's degree from KITS Warangal Kakatiya University. His Research intrests includes Reconfigurable Antenna, THz Antennas.

K Phaninder Vinay is Ph.D. in Electronics & Communication Engineering at Andhra University, Visakhapatnam, India. He is currently working as Professor in the department of ECE, Raghu Engineering College Visakhapatnam. He is professional member of IETE & IEEE. He receieved his M.Tech in Instrument Technology from Andhra University, Visakhapatnam, India. His Research intrests includes Textile Antennas, Body Worn Antennas.

Ramesh Boddu is Ph.D. in Electronics & Communication Engineering at KIIT University, Bhubaneswar, India. He is currently working as Assistant Professor in the department of ECE, Raghu Engineering College Visakhapatnam. He receieved his M.Tech in Electronics & Communication Engineering (Communication Systems) from Andhra University, Visakhapatnam, and his Bachlor's degree from JNTUK Kakinada University. His Research intrests includes Filtennas, Reconfigurable Antenna, THz Antennas.

Appendix I

S. No	Abbreviation	Description
1.	VNA	Vector Network Analyzer
2.	dB	Decibel
3.	VSWR	Voltage Standing Wave Ratio
4.	GHz	Gigahertz
5.	UMTS	Universal Mobile Telecommunications System
6.	Wi-MAX	Worldwide

		Interoperability for Microwave Access
7.	Wi-Fi	wireless fidelity
8.	IFS	Iterated Function System
9.	SIR	Stepped Impedance Resonator
10.	FR4	Flame Retardant
11.	ε_r	Relative Permittivity
12.	tanδ	Loss Tangent
13.	S_{11}	S-parameter